J. Membrane Biol. 141, 297–309 (1994)

The Journal of
Membrane
Biology

Cl^- and K^+ Channel Currents during the Action Potential in *Chara*. Simultaneous Recording of Membrane Voltage and Patch Currents

U. Homann*, G. Thiel

Pflanzenphysiologisches Institut der Universität, Untere Karspüle 2, 37073 Göttingen, Germany

Received: 4 March 1994/Revised: 11 May 1994

Abstract. Patch currents in the cell attached-mode and action potentials (AP) have been recorded simultaneously in internodal cells of *Chara corallina*. The action potentials are closely correlated with transient patch currents. With pipettes containing either 50 mM $CaCl_2$ or 100 mM KCl plus 1 or 5 mM $CaCl_2$, these transients measured up to 100 to 200 pA per patch at zero mV. Transients had a mean duration (time during which the current was ≥ half maximum peak amplitude) of about 1 sec, a maximum slope for current rising of about 400 pA sec^{-1} and a maximum rate of about 100 pA sec^{-1} for current decay, with no obvious effect of external Ca^{2+} on either of these parameters. In well-resolved recordings of current transients triggered by an action potential (AP), activities of two types of Cl^--conducting channels (15 and 38 pS) have been identified. Since activity of these channels was only observed during action potentials but not upon positive voltage steps, these channels are not directly voltage gated but point to a cytoplasmic gating factor which accumulates during excitation and propagates from excited areas to the patch. A K^+-conducting channel (40 pS) could be identified as well during an AP, when 100 mM KCl was in the pipette solution. The activity of this channel relaxed at the end of the APs with a time constant of about 3 sec. Stimulated activity of this channel is understood to cause the repolarization overshoot during the final phase of the action potential, whereas the transient activation of the Cl^- channels determines the fast voltage changes of the action potential.

Key words: Action potential — *Chara* — Cell-attached patch clamp techniques — (Single) Cl^- and K^+ channel recording

Introduction

Depolarization and repolarization during the AP of *Characean* alga are understood to be a consequence of transient activation of specific ion channels. Sequential activation of two types of ion-selective channels, namely for Cl^- and Ca^{2+}, has been proposed from voltage step/current relaxation analysis (Hope & Findlay, 1964; Beilby & Coster, 1979*a,b;* Lunevsky et al., 1983; Berestovskii, Zherelova & Kataev, 1987; Beilby, Mimura & Shimmen, 1993), ion flux analysis (Gaffey & Mullins, 1958; Kikuyama et al., 1984; Kikuyama, 1986; Reid & Tester, 1992) and optical methods (Williamson & Ashley, 1982; Kikuyama, Simada & Hiramoto, 1993). A widely accepted hypothesis was that voltage-gated Ca^{2+} channels are activated by membrane depolarization to conduct an initial net Ca^{2+} influx. The resulting rise in cytoplasmic Ca^{2+} should then be responsible for the activation of Ca^{2+}-stimulated Cl^- channels for the depolarization of the AP (Lunevsky et al., 1983; Kataev, Zherelova & Berestovskii, 1984; Berestovskii et al., 1987; Shiina & Tazawa, 1987).

The idea that K^+ channels are activated during the depolarization of the *Chara* AP to aid repolarization is controversial. Ion flux measurements have shown that the AP in *Characean* cells is indeed associated with a stimulation of K^+ efflux (Gaffey & Mullins, 1958; Oda, 1976; Kikuyama et al., 1984; Kikuyama, 1986). Prolongation of the AP by K^+ channel inhibitors in *Nitella* (Koppenhöfer, 1972; Shimmen & Tazawa, 1983) supported a role of K^+-channel activation for repolarization (Armstrong & Binstock, 1965; Hille, 1967). But although the AP augments K^+ efflux in *Chara* (Oda, 1976; Kikuyama et al., 1984; Kikuyama, 1986) K^+ channel blockers had no effects (Beilby & Coster,

* *Present address:* Department of Biological Sciences, University of London, Wye College, Wye Kent TN25 5AH, United Kingdom

Correspondence to: G. Thiel

1979*a*) or small effects (Shimmen & Tazawa, 1983) on the duration of the AP. This questioned the proposed role of enhanced K^+ channel activity during repolarization at least in this species (Beilby & Coster, 1979*a*; Shimmen & Tazawa, 1983).

K^+ fluxes are also considered to be responsible for the after-hyperpolarization in the final phase of the AP (Shimmen & Tazawa, 1983). In *Nitella* this voltage overshoot could be separated pharmacologically from the proposed K^+ current which supported the fast repolarization. This indicates the operation of at least two distinct types of K^+ channels during repolarization.

Meanwhile, patch clamp experiments in the cell-free configuration have revealed two types of Cl^- channels (Okihara et al., 1991; Okihara, Ohkawa & Kasai, 1993). The dependency of one type of Cl^- channel (chord conductance 25 pS at −100 mV in symmetrical 100 mM Cl^-) on Ca^{2+}, voltage and calmodulin makes this channel a likely candidate for the transport of the Cl^- current during depolarization of the AP (Okihara et al., 1991, 1993). Furthermore, depolarization of membrane patches in intact *Chara* cells causes transient activation of two types of Cl^- channels (Thiel, Homann & Gradmann, 1993). The voltage dependency, the activation/inactivation kinetics as well as the dependency on extracellular Ca^{2+} prompted the hypothesis that these channels carry the Cl^- current during the depolarization of the AP.

The assumption that these channels are elements of the electrical excitation is still uncertain since it is solely based on the above-mentioned parallel features between the cell AP and the single channel gating properties. Here, we report results from simultaneous measurements of the free-running membrane voltage and the associated currents through a cell-attached membrane patch. A comparable approach in animal cells has already allowed an unequivocal detection of the activity of single channels associated with the cell (e.g., Fischmeister, 1984; Mazzanti & DeFelice, 1990). In the present investigation, we were able to detect the proposed rise in activity of the two types of Cl^- channels early on in the AP, which confirmed the previous idea that a voltage-dependent activation of transient Cl^- channel activity is indeed a conductance which generates the depolarizing phase of the AP (Thiel et al., 1993). Furthermore, with 100 mM KCl in the pipette, the transient activity of a K^+-conducting channel was detected during the final repolarization phase of the AP.

Materials and Methods

Plant Material

Chara corallina Klein ex Wild was grown as reported previously (Thiel et al., 1993).

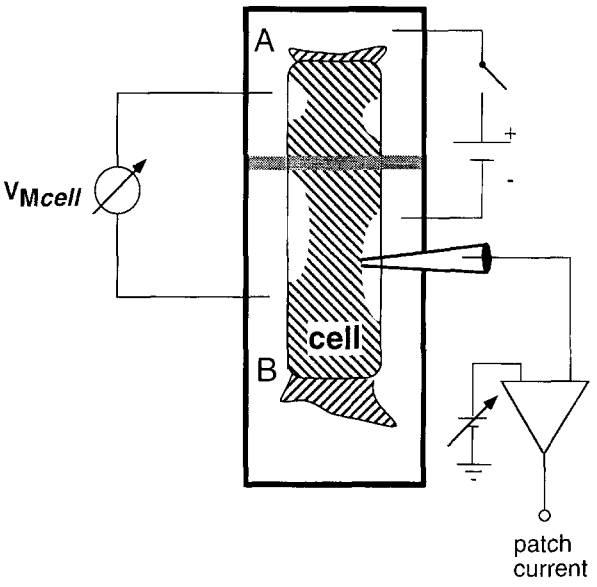

Fig. 1. Schematic diagram of the experimental arrangement (not to scale). A *Chara* internodal cell is separated by a vaseline gap (hatched bar) into two electrically isolated parts. The voltage difference between the pools *A* and *B* is measured with extracellular Ag/AgCl electrodes providing the space-averaged membrane voltage (V_{Mcell}) across the membrane in pool *B*. To trigger APs, 100 to 500 msec long current, pulses of 0.3 to 0.5 μA were applied through Ag/AgCl wires between pool *A* and *B*. A patch pipette was advanced through a small slit in the cell wall and sealed onto the plasma membrane to measure patch currents. The current was clamped at the bath voltage.

Electrical

Membrane voltage

For the combined measurement of membrane voltage (V_{Mcell}) and membrane current (Fig. 1), an internodal cell was electrically separated over a silicon gap leaving a length of approximately 1–2 cm exposed to modified artificial pond water as cell bath medium (CB) (in mM: 1 $CaCl_2$, 5 (*N*-[2-Hydroxyethyl]-piperazine-*N'*-[2-ethanesulfonic acid]) (HEPES)/NaOH, pH 7.5 and 1 (APW-1) or 3 (APW-3) KCl) in pool *B*. The other half in pool *A* was bathed in medium containing high K^+ (in mM: 1 $CaCl_2$, 5 HEPES/NaOH/pH 7.5 and 100 KCl). Sorbitol (180 mM) in *B* achieved iso-osmotic conditions between the two pools. For the required final plasmolysis (Thiel et al., 1993), additional sorbitol was added to both pools to a final concentration of 360 and 182 in pools *B* and *A*, respectively. Finally, a small slit was cut into the cell wall in regions in which the protoplast had withdrawn from the wall (Thiel et al., 1993). This was usually about 0.5 cm away from the vaseline insulation.

The free-running membrane voltage of plasmolyzed internodal cells was measured with the "K^+ anesthesia method" (Shimmen, Kikuyama & Tazawa, 1976) by the voltage between pools *A* and *B* (Fig. 1). This voltage will be the sum of the space-averaged voltages across the plasma membrane and the tonoplast of the cell part in *B* (Shimmen et al., 1976). Control measurements of the resting voltage in nonplasmolyzed cells with the K^+ anesthesia method in parallel with an intracellular microelectrode (with tip presumably located in the cytoplasm) differed by 4 ± 3 mV (4 cells) with the latter being more negative. This voltage difference, presumably the voltage across the tonoplast, was not considered in the analysis. A drawback of the K^+ anesthesia method is that the voltage record during an AP

reflects not only the desired voltage across the plasma membrane but a complex function of the plasma membrane and tonoplast action potential (Findlay & Hope, 1964). Furthermore, if the voltage in compartment B is not uniform along the entire cell segment, e.g., during a propagated AP, there will be significant deviation between a spaced-averaged voltage and the local voltage at any particular membrane patch. Control recordings of action potentials again with K^+ anesthesia and intracellular microelectrodes revealed small differences between pairs of voltage records: APs measured with intracellular electrodes (tip presumably in cytoplasm) depolarized in average 1.3 ± 4.6 mV (4 cells, $n = 35$) more positive than those recorded with K^+ anesthesia. The former APs were at an average of 0.4 ± 0.3 sec shorter than the latter. These methodological artifacts which confound an accurate current/(plasma membrane)-voltage relation during APs were minimized as follows: AP-associated single channel data were collected not only during the core of APs, but—to avoid significant contribution of the tonoplast action potential and spacial inhomogenity—also at quasi steady-state after the voltage had returned to ≥ 90% of the resting voltage (*see* Figs. 6, 7 and 8).

Because of the large surface of the *Chara* cells, capacitive patch currents during the depolarization of the cell (Fischmeister et al., 1984; Mazzanti & DeFelice, 1988) were not relevant.

In the present study, some APs occurred spontaneously. In general, they were electrically triggered by injecting a current pulse (0.3–0.5 μA, 100 to 500 msec) in pool *B* (Fig. 1).

Macroscopic Membrane Currents

Voltage step/current relaxation analysis on 1 mm long sections of intact, turgid *Chara* cells was performed according to Lunevsky et al. (1983). Voltage and current recordings were obtained with a clamp amplifier (μP, Wye Science, Wye, UK), using conventional intracellular electrodes for voltage recording. Voltage-pulse protocols, data acquisition and data analysis were controlled by a microcomputer via the pCLAMP hard- and software facilities (Axon Instruments, Foster City, CA). The space-clamped section of the *Chara* internodal cell was exposed to the same solutions used as electrolytes in patch pipettes (*see below*). The remaining cell surface was kept in APW-1.

Membrane Patch Currents

Patch currents were measured, stored and analyzed as reported previously (Thiel et al., 1993). If not stated otherwise, the pipette solutions (P) contained either (concentration/activity; in mM): 50/34 $CaCl_2$ or 100/77 KCl and 1/0.57 $CaCl_2$. The activities were calculated with appropriate activity coefficients from Robinson and Stokes (1968). Estimates of the equilibrium voltages in cell-attached measurements were obtained from the range of cytoplasmic activities reported for *Characean* alga. Values reported as concentrations were corrected with appropriate activity coefficients [number in brackets (Robinson & Stokes, 1968)] (in mM): K^+; 61 [0.8] to 117 (Beilby & Blatt, 1986); Cl^-; 2 (Coleman, 1986) to 9 [0.9] Okihara & Kiyosawa, 1988; Ca^{2+}; 2×10^{-4} (Miller & Sanders, 1987).

Since all data on membrane currents are recorded in the cell-attached mode, the membrane voltages (V_M) reflect the negative pipette voltage (V_{pip}) plus the simultaneously measured free-running membrane voltage (V_{Mcell}).

Abbreviations

AP: action potential; V_{Mcell}: free-running membrane voltage; V_{pip}: inverse pipette voltage; V_M: $V_{Mcell} + V_{pip}$; E_X, equilibrium of ion X.

Results

Figure 2 illustrates characteristic relations between membrane voltage (V_M) and currents in a plasma membrane patch of an excitable *Chara* internodal cell. The upper trace (trace *A*) shows the free-running membrane voltage (V_{Mcell}) before and during electrically triggered APs. The trace below the membrane voltage (trace *B*) presents the simultaneously recorded currents across a cell-attached plasma membrane patch. High concentrations of Ca^{2+} in the pipette (≥ 50 mM) in combination with clamp voltages (V_{pip}) positive of V_{Mcell} increased the frequency of randomly occurring outward Cl^- current transients (Thiel et al., 1993). In the present example with 50 mM $CaCl_2$ in the pipette, such a current transient was recorded while clamping the patch 100 mV positive of the free-running membrane voltage (V_M, +12 mV) (Fig. 2, trace *Bb*). The combined measurement of current and voltage shows that these transients remain restricted to the membrane patch with no perceivable effect on V_{Mcell} (Fig. 2, trace *Ab*).

Similar large currents of transient duration and with an equally fast rising and trailing kinetics could generally be activated by triggering a cell action potential. Figure 2 traces *Aa/Bb* and *Ac/Bc* (*see also* Figs. 4, 7, and 8) show two typical patch current transients which activated while the cell fired action potentials. With some exceptions (*see below*, e.g., Fig. 4) the general features of AP-generated transient current activation were similar between different patches (*see* Table). However, even within any one patch, the amplitude of the currents which activated during comparable APs varied considerably (*compare* Fig. 2 trace *Ba* and *Bc*). For example, in one comparative experiment 4 APs with similar amplitudes (ΔV_{Mcell}) 64 ± 4 mV, $n = 4$) were activated in one cell. During these APs, a mean transient outward current of 121 ± 72 pA was obtained.

After repetitive stimulation, the membrane patches abruptly lost the ability to activate the characteristic large transient currents even though the cell was still excitable. This generally occurred, depending on the patch, after 2 to 10 consecutive APs. Figure 2 trace *Ad/Bd* shows one example for such an "inactivation" of the same, previously excitable patch. In this case, the membrane turned into an "inactive" state after nine preceding APs, which all generated large transient currents in the patch (*not shown*). The remaining current response in an "inactive" patch during an AP was only a small fraction of the large current transient generally recorded during an action potential (*compare* dotted line in Fig. 2, *Ba/Bc*). Considering the seal resistance of the patch (6.8 GΩ), the membrane depolarization (ΔV_{Mcell}, 50 mV) should result in a current artifact of 7.3 pA. This predicted current is close to the peak current of 6.5 pA measured (Fig. 2, trace *Bd*), suggesting that it reflects a leak current artifact. Contribution of small

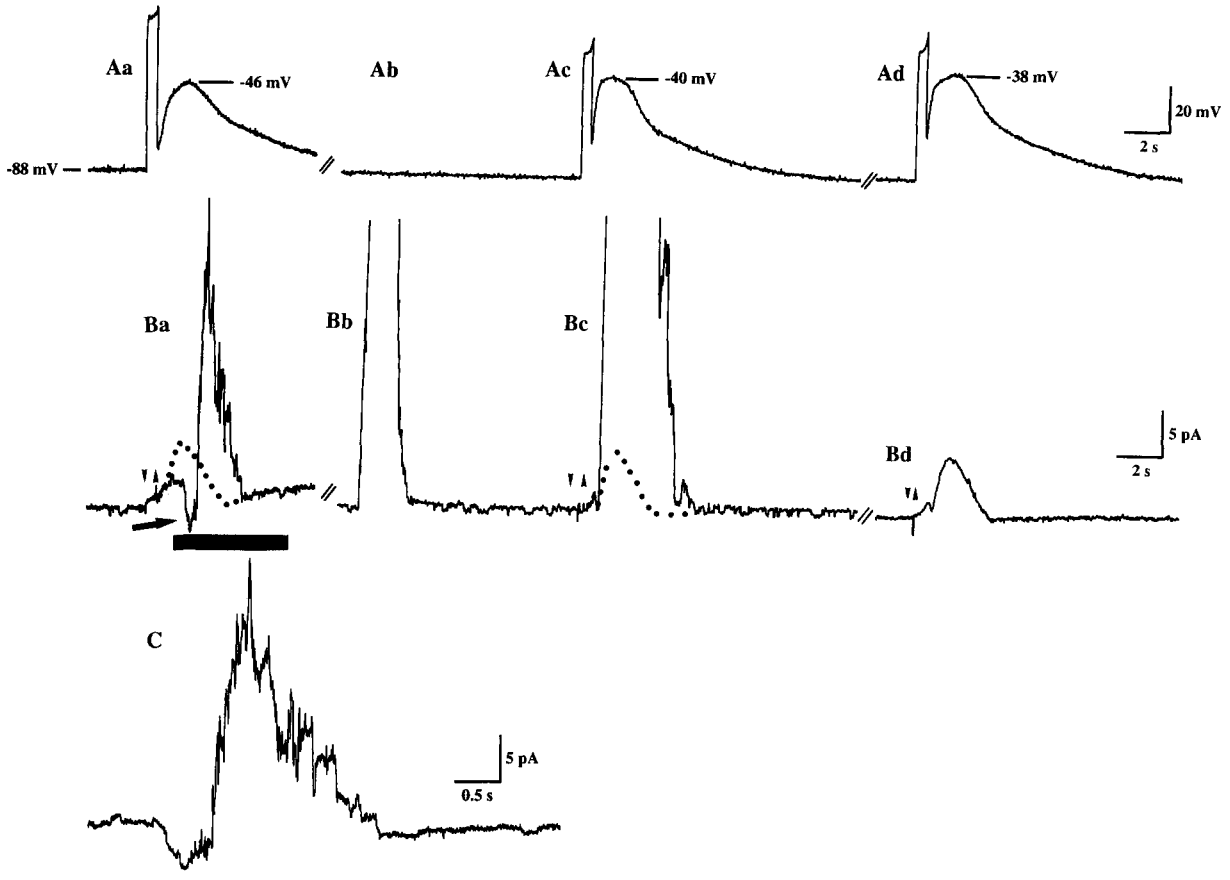

Fig. 2. Free-running membrane voltage and patch currents in cell-attached patch. Continuous trace of simultaneous measurement of V_{Mcell} (upper trace, *A*) and patch current (middle trace, *B*). Pipette solution (in mM), 50 $CaCl_2$, cell bath solution, APW-3K; seal resistance 6.8 GΩ. During electrically stimulated APs, large transient outward patch currents of variable size were recorded while holding the membrane patch (V_{pip}) 100 mV positive of the free-running membrane voltage (traces *Aa, Ba* and *Ac, Bc*). The first current response (marked section) is shown in a blow-up in trace *C*. Arrow indicates a leading inward current present in *Ba* but absent in *Bc*. Independent from cell APs (trace *Ab*), similar large transient currents occurred spontaneously under the given conditions (trace *Bb*). After nine consecutive APs, the cell was still excitable (trace *Ad*) but the membrane conducted only a small and smooth background current (traces *Ad, Bd*). For comparison, the remaining background current was drawn as dotted lines in traces *Ba* and *Bc*. Numbers at traces denote recorded V_{Mcell}. Arrowheads denote on (▼) and off (▲) switching of current pulse for AP triggering.

nonresolvable channel currents, however, cannot be excluded.

In 14 out of 56 patches there was no AP-related current activation which was significantly larger than that predictable for the leak current artifact. These patches may reflect nonexcitable membrane areas.

Initial Inward Current

A comparison of the two AP-associated outward currents shows that only the first one is preceded by a transient inward current (Fig. 2, *Ba* arrow). Due to the variable appearance of this current, a nonconsistent current-voltage relation (*data not shown*) and the absence of single channel observations, it was not investigated further.

Identification of AP-associated Currents/Channels

To obtain a current-voltage relation of the AP-associated current transients, cells were consecutively excited while clamping the membrane to a range of V_{pip} in addition to V_{Mcell}. The peak currents, obtained from four patches with 50 mM $CaCl_2$ as electrolyte, were plotted as a function of V_M (Fig. 3*A*). The large scatter of the data gives only a rough estimate of the reversal voltage at about −50 mV. The reversal voltage obtained is at the lower edge of the estimated range of Cl^- equilibrium voltages [E_{Cl^-}: −90 to −52 mV, *see* Materials and Methods] but different from the reversal voltages of other relevant ions [E_{K^+}: $-\infty$; $E_{Ca^{2+}}$: +158 mV; *see* Materials and Methods] (Fig. 3*B*). Comparable current-

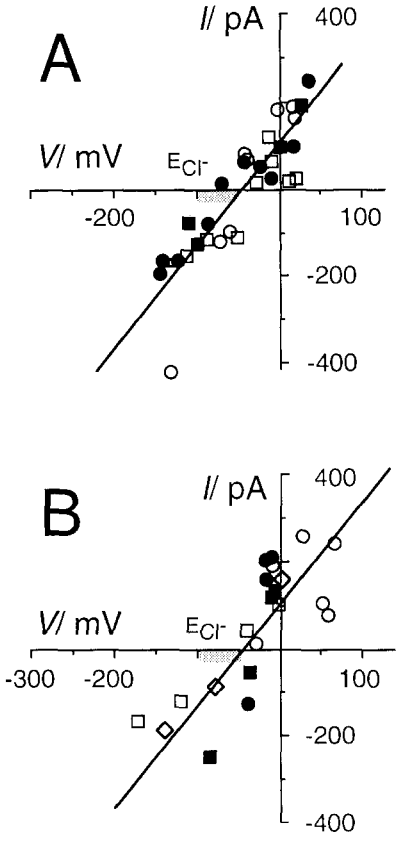

Fig. 3. AP-generated peak current as a function of V_M and pipette solution. Consecutive APs were triggered in different internodal cells (CB: APW-3K) while holding the membrane at a range of test voltages. At the same time, a cell-attached electrode measured the associated patch currents. V_M across the patch estimated as the sum of V_{pip} and V_{Mcell} at the time of the transient current peak. Currents were corrected for leak artifacts during the AP considering the seal resistance of individual patches and the corresponding ΔE_{Mcell}. Pipette solution (in mM) in *A* was 50 $CaCl_2$ and in *B*, 100 KCl, 1 $CaCl_2$ (open symbols) or 95 choline-Cl, 5 $CaCl_2$ (filled symbols). Each symbol represents a different patch. The lines in *A* and *B* were obtained by regression of the data points in *A* only. Shaded bar indicates the estimated range of equilibrium voltages for Cl^- (*see* Materials and Methods).

voltage relations were obtained in other experiments with either 100 mM KCl and 1 mM $CaCl_2$ or 95 mM choline-Cl and 5 mM $CaCl_2$ as pipette solution (Fig. 3*B*).

The assumption that Cl^- ions constitute the bulk charge of the transient currents could be confirmed on the basis of single channel step analysis. The majority of transient currents (random and AP-associated) was only resolvable, to a limited extent, as single channel steps (Fig. 2, *Ba/c; C*) in the end phase. Only in selected examples could the underlying single channel activity be resolved: Fig. 4 shows examples of current records from two patches before, during and after an electrically stimulated AP. Before stimulation, the membrane patches showed no or very little channel activity (*see also* Fig. 5). During cell excitation, the current through the membrane patches increased and remained untypically elevated even after the cell AP had returned to the resting V_{Mcell} (Fig. 4). In one extreme case, a shallow AP generated the switching of single channels with two distinct open channel amplitudes. In the other example, the currents conducted during the core of the AP still remained unresolvable but at a later state of the currents became distinguishable as switching of single channels (Fig. 4, traces *Ba, Bb*). To obtain a current-voltage relation of the AP-associated channels, the latter patch was clamped—with the induced channels still active—for about 5 sec to different V_M (post AP) (Fig. 5). In this patch and three other comparable experiments, an *I/V* relation of two distinct open channel currents (slope 15 and 38 pS) was obtained which reversed at −78 mV. This voltage is in the range [−94 to −55 mV] of the estimated Cl^- reversal voltage.

The *I/V* relation obtained for the two Cl^- channels compares well with the two open channel amplitudes resolved during the AP in Fig. 4, trace *Bb*. Furthermore, also resolvable current steps detected in AP-related transient currents (e.g., Fig. 2*B*) (Fig. 6) have a similar current-voltage relation. This stresses that the two types of Cl^- channels are the principal pathways for the transient current flow during the AP.

K^+ Channels

When the patch pipette contained KCl (P: 100 KCl, 1 mM $CaCl_2$) some APs (7 out of 20) were clearly associated—in addition to the activation of Cl^- currents—with a transient rise of K^+ channel activity. Figure 7 illustrates a combined recording of an AP and the associated current in one membrane patch. During the final phase of the repolarization, the switching of AP-generated single channel activity was resolvable, fading out within 12 sec after onset of cell excitation.

The linear *I/V* relation of the open channel (40 pS slope conductance) was obtained directly as a function of V_M (Fig. 7). A channel with a comparable unitary conductance was found in six other patches during the late phase of the AP (data summarized in Fig. 7*D*). The channel amplitudes obtained from these measurements were well fitted by the same linear *I/V* relation obtained in the example above.

The extrapolated reversal voltage is at the positive margin for the range of expected reversal voltages for K^+ [−11 to +6 mV] (Fig. 7*C*), while the equilibrium voltage for other relevant ions (Ca^{2+}, Cl^-) is outside this range. Thus, these AP-associated channels must carry K^+ ions [E_{Cl^-}: −94 to −55 mV; $E_{Ca^{2+}}$: +100 mV; *see* Materials and Methods].

In all patches in which the AP-associated K^+ channels were observed, they completely inactivated within 20 to 30 sec after activation of the Cl^- currents. Figure 8 shows the inactivation of K^+ channels from one

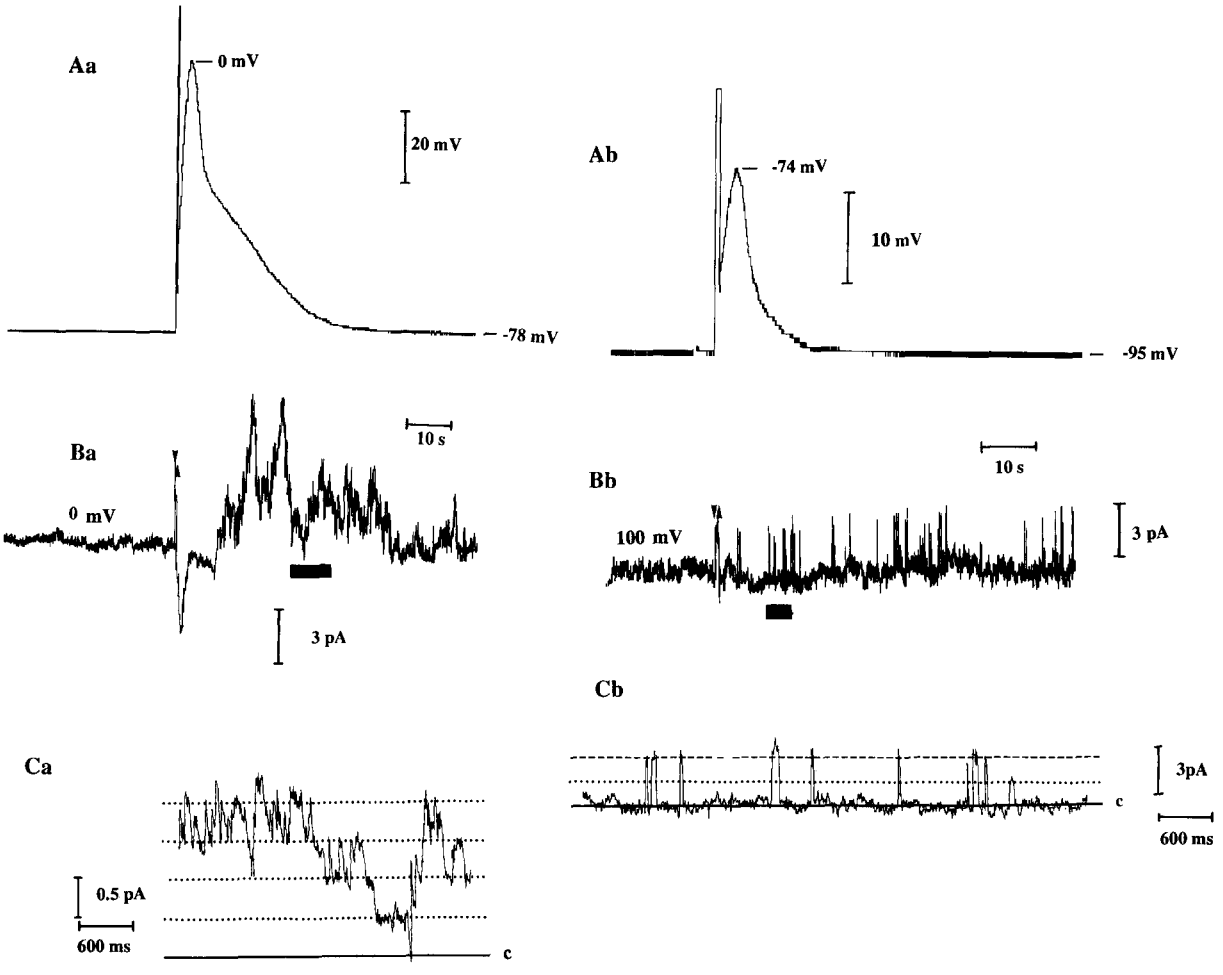

Fig. 4. AP-associated activation of channel activity. In two internodal cells (CB: APW-3K) APs (*Aa–b*) were electrically triggered and the patch currents (P: 100 KCl, 1 $CaCl_2$) (*Ba* and *Bb*) measured at the same time with electrodes sealed to the plasma membrane. Numbers at the voltage trace denote V_{Mcell} measured and numbers at current trace give V_{pip}. Panels *Ca* and *Cb* show blow-ups of sections marked in *Ba* and *Bc*. Unbroken lines indicate baseline current (*c*) with all channels closed. Dotted and dashed lines mark discrete levels of unitary open channel currents. Arrowheads denote on (▼) and off (▲) switching of current pulse for AP triggering.

patch in the late phase of one of four spontaneous APs. An exponential equation ($I(t) = Io\ e^{(-t/\tau)}$) was fitted to the current relaxation starting 7 sec after onset of the outward current. This operation provided a time constant of 2.1 ± 1.2 sec for K^+ channel inactivation in the 4 APs. The same analysis conducted in four other patches with the same inactivating K^+ channel revealed a similar mean time constant of 2.5 ± 1 sec (n = 7).

Effect of Ca^{2+} in Pipette on AP-associated Cl^- Transients

AP-associated Cl^- current transients were triggered no matter whether the pipette contained 1, 5 or 50 mM Ca^{2+} (Figs. 2, 4 and 8). This is in stark contrast to the Ca^{2+} requirement for the random activation of Cl^- transients (Thiel et al., 1993). These were only activated with ≥50 mM Ca^{2+} in the pipette. To quantify the effect of extracellular Ca^{2+} on Cl^- channel activation, AP-associated currents were recorded in five different patches with either 5 or 50 mM Ca^{2+} in the pipette. To increase the quantitative comparability of the AP-generated currents between different patches, V_{pip} was held at 0 mV and only APs with similar amplitudes were considered for analysis. The results, which are summarized in the Table, show that a tenfold increase in Ca^{2+} in the pipette had no perceivable effect on the peak amplitudes of AP-generated outward currents. Further inspection of the AP-generated outward transients showed that extracellular (pipette) Ca^{2+} had also no obvious effect on the features of current rising and trailing kinetics nor on the mean duration of transient current activity (Table, *A*).

The rising and trailing kinetics of AP-generated transients were also analyzed in a greater number of patches without considering differences in AP ampli-

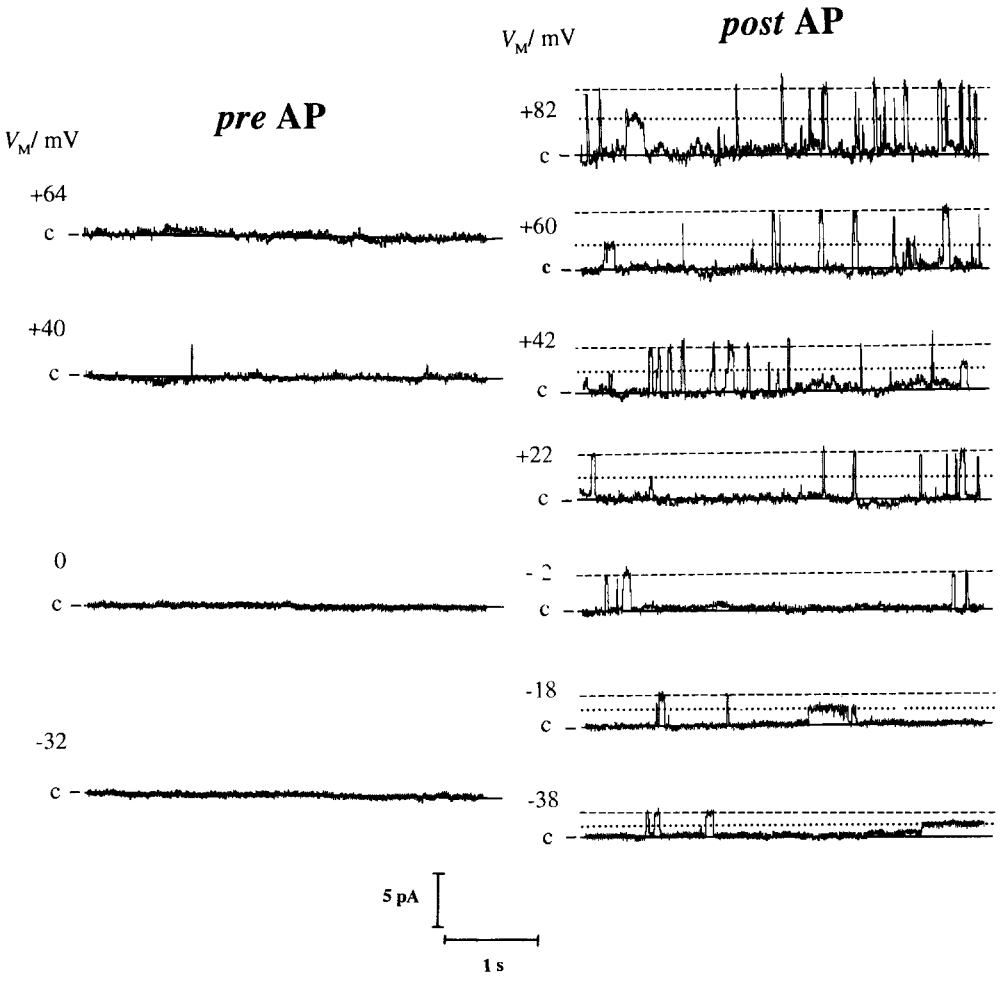

Fig. 5. Unitary open channel currents from channels activated as a consequence of the AP shown in Fig. 4, trace *Aa/Ba*. Before triggering the AP, the patch showed no perceivable channel activity (pre-AP). Over some minutes after excitation (post-AP), two different types of channels were recorded at different V_M (numbers on left of traces denote V_M as a sum of V_{pip} and V_{Mcell}). Baseline with channels closed (unbroken line) is indicated by *c*. Levels of open channel currents of the two types of channels are indicated by dashed and dotted lines.

tudes, V_{pip} and pipette electrolyte (Table, *B*). The kinetic values are similar to those obtained under restricted conditions in Table, *A*.

Temporal Relation between Cell AP and Cl^- Transient Patch Current

In the present study, AP-associated Cl^- current transients could significantly lag behind the onset of the cell AP. An example for a clear lag time (about 5 sec) between onset of the AP and current activation is illustrated in Fig. 8*A*. The reason for the latency could be propagation of the AP to the patch. Alternatively, the variable lag times could be due to kinetic constraints of channel activation reflecting a randomness in Cl^- channel gating. To analyze further the temporal relation between cell excitation and transient current activation, the AP peak was plotted against the corresponding Cl^- current peak (Fig. 9). The data show a correlation between the occurrence of the AP peak and the current peak.

Whole-Cell Excitation Currents

For a quantitative comparison between AP-generated current transients across membrane patches and macroscopic currents conducted during an action potential voltage step/current relaxation, experiments on intact cells were performed. Figure 10 shows the current response of a space-clamped *Chara* membrane rinsed in 50 mM $CaCl_2$. The membrane was depolarized in a step from the resting voltage (−104 mV) to 0 mV. The first step resulted in an activation of the typical transient excitation currents (*compare* Lunevsky et al., 1983). A following second step during the refractory period only activated the nonexcitatory background currents. The

current difference between the peak current of the first step and the corresponding current during the second (refractory) step was collected from comparable experiments in four different cells (Fig. 10*B*). The mean current density of the peak outward current measured at 0 mV in these cells was 3.9 ± 1.3 (20 APs, four cells). There was no significant difference in the peak current density or activation/inactivation kinetics (on the 99% confidence level) after replacing in two cells the bath solution (50 mM $CaCl_2$) by a medium containing 95 mM choline-Cl and 5 mM $CaCl_2$ (*not shown*).

Discussion

Membrane excitation in *Chara* cells causes a transient enhanced efflux of KCl across the plasma membrane (Oda, 1976; Kikuyama et al., 1984; Kikuyama, 1986). In the present study, two distinct Cl^- channels and one K^+ channel, which transiently activate in the course of a cell AP, were identified. The short-lasting activation of these channels must therefore reflect the elementary mechanism responsible for the transient rise in KCl efflux during excitation.

The initial inward current leading the activation of some Cl^- outward current transients (e.g., Fig. 2) needs further investigation with respect to a postulated Ca^{2+} current early on in the AP (Lunevsky et al., 1983). For a more precise investigation of this initial current voltage step/current relaxation, experiments with space-clamped cells should be more promising.

Properties of Cl^- Channels/Currents

The properties of the two AP-associated Cl^- channels are similar to those found to activate randomly in positive-clamped cell-attached patches (Thiel et al., 1993). The channels compare well with respect to the unitary channel conductance, transient activity, current rise/trailing kinetics as well as with channel density. The present study therefore confirms the hypothesis that the previously described gating properties of these channels, which depend on voltage and extracellular Ca^{2+}, play a principal role in voltage-triggered membrane excitation (Thiel et al., 1993).

Voltage step/current relaxation measurements on intact cells bathed in 50 mM $CaCl_2$ revealed at 0 mV clamp voltage a peak excitation current of 3.9 ± 1.3 A m^2. This value can be directly compared to the peak Cl^- currents across the patches because both currents were recorded with the same extracellular/pipette solution. AP-induced patch currents measured on average about 100 pA per patch at 0 mV (Fig. 3). Considering a patch area of approximately 10 μm^2 (Mazzanti & DeFelice, 1988), this current density extrapolates to a whole-cell current density of 10 A m^2. This estimated value is in good agreement with the currents measured in intact cells. The small difference between the values can be explained when considering nonexcitable areas in the membrane (about 25%, *see above*) and/or an uncertainty in the patch area estimate.

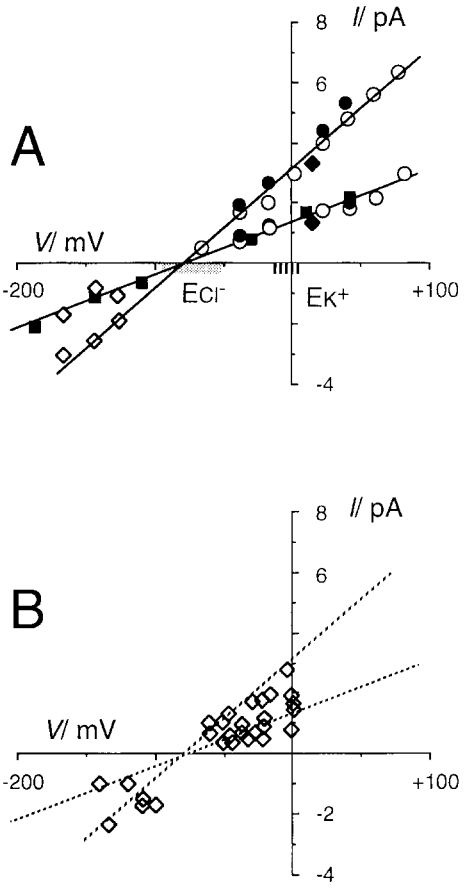

Fig. 6. Current-voltage (*I/V*) relation of AP-generated Cl^- channel activity. Open channel currents obtained by plotting discrete current steps from Fig. 4, trace *Bb* (◆), Fig. 5 (○) and three comparative experiments (remaining symbols). The lines are obtained by regression of the data points. Reversal voltage for both fits −78 mV; slope conductance 15 and 38 pS. Equilibrium voltages (E_{Cl^-} and E_{K^+}) which are relevant in the illustrated voltage range are indicated by shaded bars (*see* Materials and Methods). Current-voltage relation of resolvable current steps from the trailing phase of different AP-generated current transients (nine patches) (*B*). The dotted lines were obtained from the regression in *A*.

Mode of Cl^- Channel Activation

In line with previous findings (Thiel, MacRobbie & Hanke, 1990; Thiel et al., 1993) the present data support the notion that a cytoplasmic gating factor activates Cl^- channels. Although patches unequivocally contained excitable Cl^- channels, they were not activated by clamping the membrane patch positive (e.g., Fig. 5). This renders an immediate voltage gating of the Cl^-

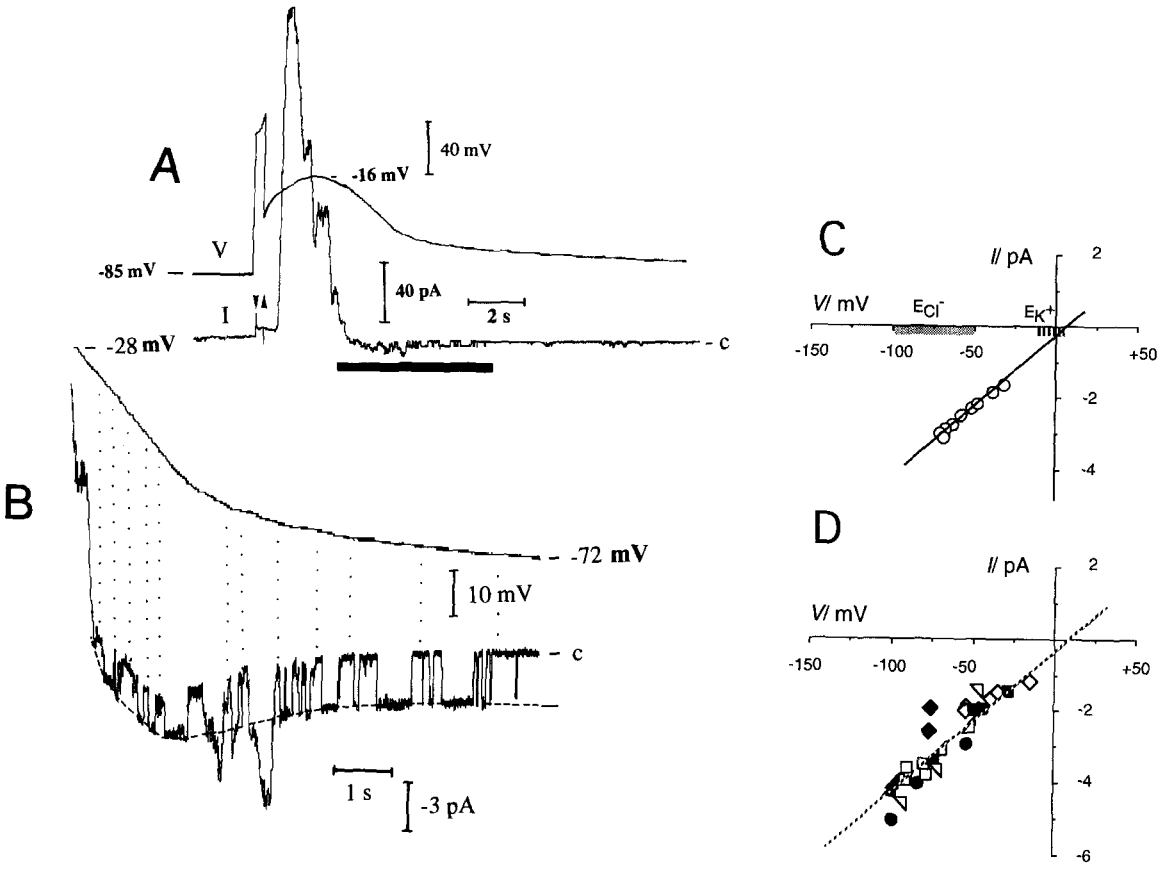

Fig. 7. Characterization of K^+ channel activity during the late phase of an AP. (*A*) Electrically triggered AP (*V*) and the associated patch currents (*I*) (P: 100 KCl, 1 $CaCl_2$; CB: APW-3K). The final phase of membrane repolarization is associated with a decrease in single channel activity. A blow-up of the section marked (filled bar) is illustrated in *B*. The current-voltage relation of the open channel is obtained by a direct correlation of V_M (V_{pip}, 0 mV) as indicated by dotted lines. Estimated open channel level indicated by dashed line. (*C*) The regression line through data points from *A* extrapolates through a reversal voltage of +7 mV; slope conductance 40 pS. Equilibrium voltages (E_{Cl^-} and E_{K^+}) which are relevant in the illustrated voltage range are indicated by shaded bars (*see* Materials and Methods). (*D*) Collected *I/V* data of AP-associated open channels from six other patches (each patch represented by different symbols); currents measured at quasi steady-state ($\geq$ 90% repolarization of cell resting voltage) V_{Mcell} and different V_{pip}. The dotted line is the regression line from *C*. Arrowheads denote on (▼) and off (▲) switching of current pulse for AP triggering.

channels in the patch impossible. Thus, the underlying mechanism for activation of an action potential in *Chara* must require more components than voltage as a trigger. Also, for the above reasons, a simple voltage-dependent rise of a net Ca^{2+} influx through the membrane patch appears not to account for the Cl^- channel activation in the patch.

The gating of AP-generated Cl^- channel activity is consistent with the interpretation that the activation in the membrane patch is due to a diffusion of a cytoplasmic gating factor—possibly Ca^{2+} (Thiel et al., 1993)—from adjacent, excited membrane areas to the region of the patch. The close relationship between the time course of the cell AP and the activation of the Cl^- currents (Fig. 9) support the view that the same constraints which determine the whole-cell action potential and its propagation are essential for the transient activation of Cl^- channels as well. Furthermore, while positive voltages across a membrane patch resulted in an activation of randomly occurring Cl^- transients (Thiel et al., 1993) the activation of AP-associated currents is more predictable (Fig. 9). The latencies of Cl^- current transient activation after AP triggering clustered around a mean value within any one patch. This also fosters the idea that channel activation is indirectly caused by the influence of adjacent excited membrane areas.

This very difference between AP-generated and randomly activated Cl^- currents gives further insight into the gating mode of the channels: i.e., the activation step responsible for the randomness of activation is not imminent to the Cl^- channels. It must be the consequence of preceding steps in the voltage- and Ca^{2+}-dependent activation scenario.

While the channels in the membrane patch can apparently be activated from adjacent excited membrane regions, the reverse does not seem possible. Conse-

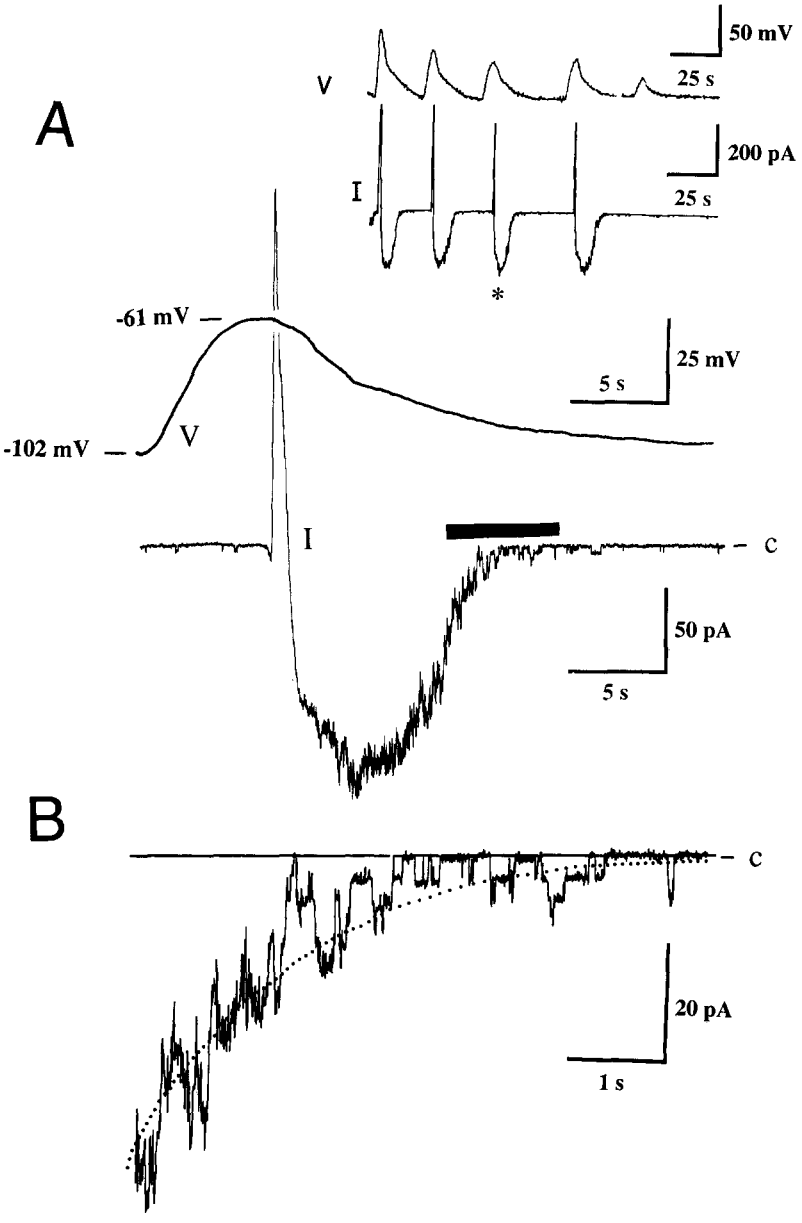

Fig. 8. Kinetics of K^+ channel inactivation in the end phase of cell AP. Simultaneous recording of a train of five spontaneous APs (*V*) with the corresponding patch currents (*I*) (*inset*, upper right) (P: 100 KCl, 5 $CaCl_2$; CB: APW-1K). (*A*) Blow-up of the AP (*V*) and current (*I*) marked by an asterisk in inset. The final phase of the AP-generated transient current is characterized by decreasing activity of the 40 pS K^+ channel. A further blow-up of the section marked (filled bar) in *A* is shown in *B*. Baseline current (*c*) with all channels closed is indicated by unbroken line. The dotted line gives the exponential fit (time constant 1.6 sec) of the form $I(t) = Io\ e^{(-t/\tau)}$ to the current measured ≥7 sec after onset of the outward current.

quently, the local rise of an activating factor, sufficient to activate multiple Cl^- channels in the patch, is not sufficient to cause excitation of neighboring membrane regions. Thus, electrical propagation of the depolarization along the membrane surface, which is in the present situation inhibited by the seal resistance, is the prime mechanism for AP propagation.

A comparison of the current rising and trailing kinetics of randomly activated Cl^- transients and AP-associated transients exhibits no obvious difference between both activation modes. This result indicates that the current rising/trailing kinetics are not voltage dependent, i.e., the kinetics are similar whether the whole cell is excited or not. Similarly, the randomly activating Cl^- currents also revealed no obvious voltage dependency (Table) (Thiel et al., 1993). In conclusion, the data show that, although the activation of the transient currents is voltage dependent (Thiel et al., 1993), the kinetics are not. The interpretation is that voltage affects an all-or-none mechanism leading to channel activation while the final control of the coordinated channel activation and inactivation is then under a voltage independent, intrinsic control. Since the current rising and trailing features are comparable between cells, the mechanism must be conservative. Notably, the mean activation time of Cl^- current transients of about 0.9 sec (Table) is very similar to the mean duration (about 1.2 sec; for the time during which the current was ≥ half maximal voltage amplitude) of macroscopic APs obtained from a large number of *Chara* cells (Fig. 12, Beilby & Coster, 1979*b*). Thus, it can be concluded that the conservative rising and trailing kinetics of the Cl^- cur-

Table. Kinetic parameters of AP-triggered outward current transients.

Pipette medium (mM)	V_{pip} (mV)	Resting-V_{Mcell} (mV)	Peak AP-V_{Mcell} (mV)	pc (pA)	t (sec)	rt (pA sec^{-1})	tt (pA sec^{-1})	rt/tt	n
A									
95 choline Cl 5 $CaCl_2$	0	−108 ± 9	12 ± 18	154 ± 35	0.86 ± 0.2	829 ± 255	191 ± 50	4.3 ± 1.7	6
50 $CaCl_2$	0	−96 ± 9	10 ± 9	102 ± 41 [0.04]	0.86 ± 0.2	410 ± 293 [0.04]	149 ± 40 [0.18]	2.4 ± 2.1 [0.11]	5
B									
50 $CaCl_2$ or 95 chol.Cl 5 $CaCl_2$	$0 \leq V_{pip} \leq 100$				0.9 ± 0.4	383 ± 406	93 ± 75	3.6 ± 2.9	59

(A) Effect of tenfold difference in Ca^{2+} in the pipette on peak currents, rising and trailing kinetics and mean duration of transient current activity. The peak current (pc) measured as AP-generated positive current deflection from baseline current. Current rising (rt) and trailing (tt) estimated as rate of ΔI between 10 and 90% of total current from the baseline to the peak (rising) and back (trailing). Mean duration (t) of transient currents estimated as time during which the current was ≥ half of the maximum peak current. Numbers in brackets give confidence limit (from Student t-test) for the hypothesis that mean values of the respective columns are different. (B) Data for t, rt and tt as in A but pooled from 18 patches not considering differences in pipette solution, AP amplitudes and V_{pip}.

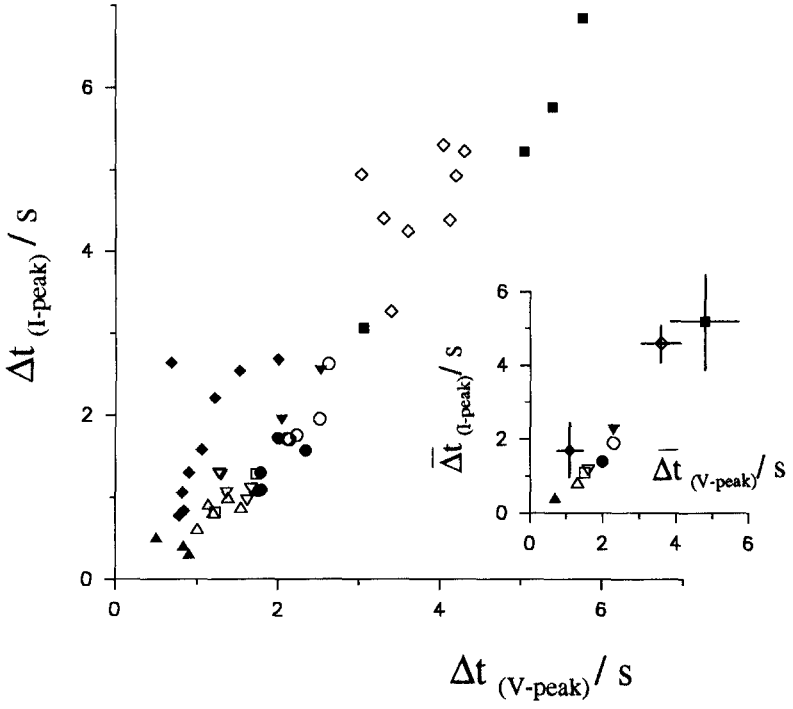

Fig. 9. Temporal relationship between cell AP and Cl^- current transient. Plot of the latencies for AP peaks *vs.* peak of the associated Cl^- current transient. Data from 10 patches with 4 to 7 APs within each experiment (not considering differences in V_M and pipette electrolyte). Latency times obtained from the time difference between respective peaks and the turning off of the triggering stimulus or onset of spontaneous AP. *Inset:* mean values for data with respect to individual patches. Bars show SD if larger than symbol.

rent transients alone are sufficient to explain the macroscopic features of the fast voltage changes during excitation. This is consistent with the absence of an effect of K^+ channel blockers on the time course of the fast phase of the AP in *Chara* (Beilby & Coster, 1979*a*; Shimmen & Tazawa, 1983).

Along with the yet unknown gating factor responsible for channel activation, the Cl^- channels must have at least one other superordinated control site reflected by the transition of patches into an inactive state after a series of APs (Fig. 2). This is in line with reports which have indicated protein phosphorylation/dephosphorylation and Ca^{2+}-calmodulin dependent control of membrane excitation (Tsutsui et al., 1987; Shiina et al., 1988; Okihara et al., 1991, 1993). The inactivation of patches would not be expected from the whole-cell level, as *Characean* cells are generally excitable many more times over (e.g., Kishimoto, 1966). It may be speculated that a pleb formation of the membrane in the patch (Milton & Cadwell, 1990) results in an AP-dependent local depletion of an essential factor for channel activation.

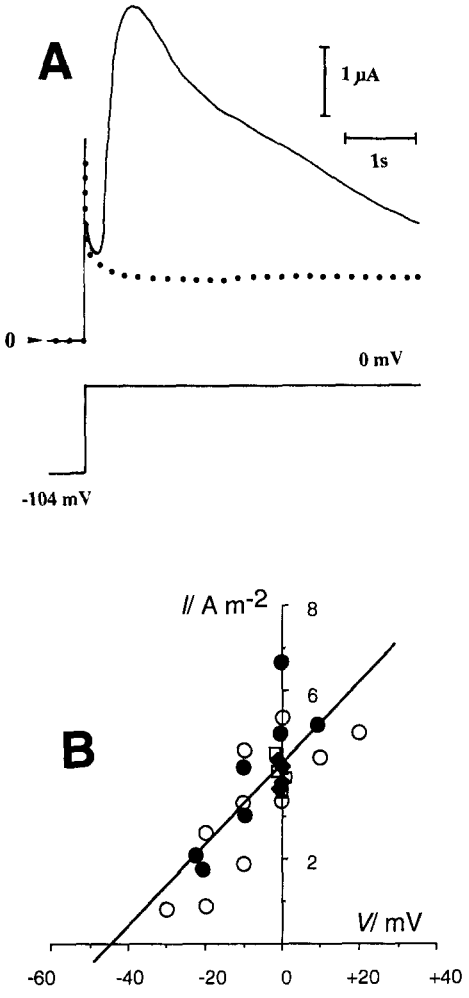

Fig. 10. Macroscopic current responses of space-clamped *Chara* internodal cells to depolarizing test voltages. (*A*) A voltage step from the resting voltage (−104 mV) to 0 mV resulted in a space-clamped cell segment (1 mm long) exposed to 50 mM $CaCl_2$ in an activation of a transient excitation current (unbroken line). The same clamp steps during a refractory period (about 1 sec after release of the initial clamp) resulted in the activation of a constant background current (dotted line). (*B*) Summary of peak current responses (excitation current minus current during refractory period) obtained in four cells as a function of the clamp voltage. Different symbols represent different cells.

Properties of K^+ Channel

The present study confirms and further details an earlier hypothesis that the AP in *Characean* algae is associated with a rise in K^+ conductance (Shimmen & Tazawa, 1983). The contribution of K^+ channel activity during the fast repolarization remains uncertain because potential K^+ channel activity in the early phase of the AP was masked by the large Cl^- currents. However, the temporal features of K^+ channel inactivation in the late phase of the AP support the view that K^+ fluxes contribute to the final phase of repolarization.

Depending on the position of the free-running membrane voltage with respect to E_{K^+}, inactivation of K^+ channel activity will result in a retarded repolarization ($V_M < E_{K^+}$) or a transient voltage overshoot (after-hyperpolarization) ($V_M > E_{K^+}$). Based on measurements of the whole-cell membrane resistance and on pharmacological data, Shimmen and Tazawa (1983) suggested that in *Nitella* the inactivation of a K^+ conductance is responsible for the course of the after-hyperpolarization. This voltage overshoot decays over some 10 sec with a time constant of about 15 to 20 sec back the pre-AP resting voltage (*compare* Fig. 1 in Shimmen & Tazawa, 1983). The lower time constant obtained in the present patch measurements suggests that the decay of K^+ channel activity is not solely responsible for the time course of the membrane voltage overshoot. A slower inactivation of a fraction of the activated Cl^- channels (e.g., Fig. 4) may be a limiting factor in the time course of the after-hyperpolarization. Alternatively, the ionic composition of the pipette medium may modulate K^+ channel inactivation. This interpretation finds a parallel in the effect of extracellular K^+ and Ca^{2+} on the voltage overshoot in *Nitella* (Shimmen & Tazawa, 1983). Finally, voltage measurements in giant cells such as *Characean* alga provide, to some extent, a space-averaged membrane voltage, even with intracellular micropipettes. Hence, the slower time constant from whole-cell measurements could be the consequence of nonsynchronized K^+ channel inactivation over a space considerably larger than a patch.

The close association of the K^+ channel activity with the AP suggests that K^+ and Cl^- channels are activated by a common mechanism. The presence of a Ca^{2+}-activated K^+ current in *Chara* points to a rise in cytoplasmic Ca^{2+} as a common activating step for both currents (Thiel et al., 1990).

Previously, it has been suggested that the voltage dependency of K^+ channels is responsible for channel activation during the AP (*reviewed in* Tester, 1990). For the plasma membrane of *Nitellopsis,* a K^+-selective channel with a conductance of about 50 pS and an outward rectifying open probability has been reported (Azimov, Geletyuk & Berestovskii, 1987). With respect to the unitary conductance, this channel could be the same K^+ channel found to activate during the AP. The voltage-dependent gating would support the view that membrane depolarization during the AP is responsible for channel activation. However, within a very heterogenous population of K^+ channels found in the plasma membrane of *Chara* (U. Homann, G. Thiel and D. Gradmann, *in preparation*) there was as yet no evidence for a dominant channel with a corresponding voltage-dependent open probability (Coleman, 1986; Katsuhara, Mimura & Tasawa, 1990; Laver, 1991; Thiel et al., 1993). Against this background, it is uncertain which mechanism is responsible for the activation of the 40 pS channel during the AP. But now that the combined voltage and current measurements have unequiv-

ocally identified the unitary conductance of the AP-associated K^+ channel, the gating of this channel can be investigated in more detail.

The financial support by the Deutsche Forschungsgemeinschaft is gratefully acknowledged. The authors thank Prof. D. Gradmann for constructive and stimulating criticism and J. Blatt for help in preparing the manuscript.

References

Armstrong, C.M., Binstock, L. 1965. Anomalous rectification in the squid giant axon injected with tetraethylammonium chloride. *J. Gen. Physiol.* **48:**859–872

Azimov, R.R., Geletyuk, V.I., Berestovskii, G.N. 1984. Single potential-dependent K^+ channel of the cells of the alga *Nitellopsis obtusa*. *Biofizika* **32:**79–84

Beilby, M.J., Blatt, M.R. 1986. Simultaneous measurements of cytoplasmic K^+ concentration and plasma membrane electrical parameters in single samples of *Chara corallina*. *Plant Physiol.* **82:**417–422

Beilby, M.J., Coster, H.G.L. 1979*a*. The action potential in *Chara corallina* II. Two activation-inactivation transients in voltage clamps of the plasmalemma. *Aust. J. Plant Physiol.* **6:**323–325

Beilby, M.J., Coster, H.G.L. 1979*b*. The action potential in *Chara corallina* III. The Hodgkin-Huxley parameters for the plasmalemma. *Aust. J. Plant Physiol.* **6:**337–353

Beilby, M.J., Mimura, T., Shimmen, T. 1993. The proton pump, high pH channels, and excitation: voltage clamp studies of intact and perfused cells of *Nitellopsis obtusa*. *Protoplasma* **175:**144–152

Berestovskii, G.N., Zherelova, O.M., Kataev, A.A. 1987. Ionic channels in characean algal cells. *Biofizika* **32:**1011–1027

Coleman, H.A. 1986. Chloride currents in *Chara*—A patch-clamp study. *J. Membrane Biol.* **93:**55–61

Findlay, G.P., Hope, A.B. 1964. Ionic relations of cells of *Chara australis*. VII. The separate electrical characteristics of the plasmalemma and tonoplast. *Austr. J. Biol. Sci.* **17:**62–77

Fischmeister, R., DeFelice, L.J., Ayer, R.K., Levi, R., DeHaan, R.L. 1984. Channel currents during spontaneous action potentials in embryonic chick heart cells. *Biophys. J.* **46:**267–272

Gaffey, C.T., Mullins, L.J. 1958. Ion fluxes during the action potential in *Chara*. *J. Physiol.* **144:**505–524

Hille, B. 1967. The selective inhibition of delayed potassium currents in nerve by tetraethylammonium ion. *J. Gen. Physiol.* **50:**1287–1302

Hope, A.B., Findlay, G.P. 1964. The action potential in *Chara*. *Plant Cell Physiol.* **5:**377–379

Kataev, A.A., Zherelova, O.M., Berestovskii, G.N. 1988. Effect of charged local anaesthetics on inactivation of Ca^{2+}-activated Cl^- channels of *Characean* algae. *Biofizika* **33:**1076–1084

Katsuhara, M., Mimura, T., Tazawa, M. 1990. ATP-regulated ion channels in the plasma membrane of a Characeae alga *Nitellopsis obtusa*. *Plant Physiol.* **93:**343–346

Kikuyama, M. 1986. Ion effluxes during excitation of *Characeae*. *Plant Cell Physiol.* **27:**1213–1216

Kikuyama, M., Oda, K., Shimmen, T., Hayama, T., Tazawa, M. 1984. Potassium and chloride efflux during excitation of *Characean* cells. *Plant Cell Physiol.* **25:**965–974

Kikuyama, M., Simada, K., Hiramoto, Y. 1993. Cessation of cytoplasmic streaming follows an increase of cytoplasmic Ca^{2+} during action potential in *Nitella*. *Protoplasma* **174:**142–146

Kishimoto, U. 1966. Repetitive action potentials in *Nitella* internodes. *Plant Cell Physiol.* **7:**547–558

Koppenhöfer, E. 1972. Die Wirkung von Kupfer, TTX, Cocain und TEA auf das Ruhe- und Aktionspotential von *Nitella*. *Pfluegers Arch.* **336:**299–309

Laver, D.R. 1991. A surgical method for accessing the plasma membrane of *Chara australis*. *Protoplasma* **161:**79–84

Lunevsky, V.Z., Zherelova, O.M., Vostrikov, I.Y., Berestovskii, G.N. 1983. Excitation of *Characeae* cell membranes as a result of activation of calcium and chloride channels. *J. Membrane Biol.* **72:**43–58

Mazzanti, M., DeFelice, L.J. 1988. K channel kinetics during the spontaneous heart beat in embryonic chick ventricle cells. *Biophys. J.* **54:**1139–1148

Mazzanti, M., DeFelice, L.J. 1990. Ca channel gating during cardiac action potentials. *Biophys. J.* **58:**1059–1065

Miller, A.J., Sanders, D. 1987. Depletion of cytosolic free calcium induced by photosynthesis. *Nature* **326:**397–400

Milton, R.L., Cadwell, J.H. 1990. How do patch clamp seals form? *Pfluegers Arch.* **416:**758–765

Oda, K. 1976. Simultaneous recording of potassium and chloride efflux during an action potential in *Chara corallina*. *Plant Cell Physiol.* **17:**1085–1088

Okihara, K., Ohkawa, T.A., Kasai, M. 1993. Effect of calmodulin on Ca^{2+}-dependent Cl^--sensitive anion channels in the *Chara* plasmalemma: a patch clamp study. *Plant Cell Physiol.* **34:**75–82

Okihara, K., Kiyosawa, K. 1988. Ion composition of the *Chara* internode. *Plant Cell Physiol.* **29:**21–25

Okihara, K., Ohkawa, T., Tsutsui, I., Kasai, M. 1991. A calcium-dependent and voltage-dependent chloride-sensitive anion channel in the *Chara* plasmalemma: a patch-clamp study. *Plant Cell Physiol.* **32:**593–602

Robinson, R.A., Stokes, R.H. 1968. Electrolyte Solutions. Butterworth Scientific Publications, London

Reid, R.J., Tester, M. 1992. Measurements of Ca^{2+} fluxes in intact plant cells. *Philos. Trans. R. Soc. Lond. B. Biol. Sci.* **338:**73–82

Shiina, T., Tazawa, M. 1987. Demonstration and characterization of Ca^{2+} channel in tonoplast free cells of *Nitellopsis obtusa*. *J. Membrane Biol.* **96:**263–276

Shiina, T., Wayne, R., Tung, H.Y.L., Tazawa, M. 1988. Possible involvement of protein phosphorylation/dephosphorylation in the modulation of Ca^{2+} channel in tonoplast-free cells of *Nitellopsis*. *J. Membrane Biol.* **102:**255–264

Shimmen, T., Kikuyama, M., Tazawa, M. 1976. Demonstration of two stable potential states of plasmalemma of *Chara* without tonoplast. *J. Membrane Biol.* **30:**249–270

Shimmen, T., Tazawa, M. 1983. Activation of K^+-channel in membrane excitation of *Nitella axilliformis*. *Plant Cell Physiol.* **24:**1511–1524

Tester, M. 1990. Plant ion channels: whole-cell and single-channel studies. *New Phytol.* **114:**305–340

Thiel, G., Homann, U., Gradmann, D. 1993. Microscopic elements of electrical excitation in *Chara:* Transient activity of Cl^- channels in the plasma membrane. *J. Membrane Biol.* **134:**53–66

Thiel, G., MacRobbie, E.A.C., Hanke, D.E. 1990. Raising the intracellular level of inositol 1,4,5-trisphosphate changes plasma membrane ion transport in *Characean* algae. *EMBO J.* **9:**1737–1741

Tsutsui, I., Ohkawa, T., Nagai, R., Kishimoto, U. 1987. Role of calcium ion in the excitability and electrogenic pump activity of the *Chara corallina* membrane: I. Effects of La^{3+}, verapamil, EGTA, W-7 and TFP on the action potential. *J. Membrane Biol.* **96:**65–74

Williamson, R.E., Ashley, C.C. 1982. Free Ca^{2+} and cytoplasmic streaming in the alga *Chara*. *Nature* **296:**647–651